

Cascade in Muonic and Pionic Atoms with $Z = 1$

V. E. MARKUSHIN

Paul Scherrer Institute, CH-5232 Villigen, Switzerland

December 2, 1998

Invited talk at EXAT-98, Ascona, July 19–24, 1998
(to be published in *Hyperfine Interactions*)

Abstract

Recent theoretical and experimental studies of the exotic atoms with $Z = 1$ are reviewed. An interplay between the atomic internal and external degrees of freedom is essential for a good description of the atomic cascade. The perspective of *ab initio* cascade calculations is outlined.

1 Introduction

When heavy negative particles (μ^- , π^- , \bar{p} , etc.) stop in matter, they usually form exotic atoms in highly excited states with principal quantum number $n \sim \sqrt{m/m_e}$ where m is the reduced mass of the exotic atom and m_e is the electron mass. The exotic-atom formation is followed by an atomic cascade consisting of multistep transitions to lower atomic states. For hadronic atoms, the atomic cascade is a complete life history because the hadrons get absorbed by the nuclei with high probability before reaching the ground state. Muonic atoms (where the absorption is weak) de-excite to the ground state and engage in various reactions (muon catalyzed fusion, muon transfer, molecular formation) with initial conditions determined by the atomic cascade. In both cases, the atomic cascade can reveal important information about the properties of exotic atoms and reactions with atoms in excited states. This paper, supplementing the earlier reviews [1–4], focuses on the recent progress in theoretical studies of the atomic cascade in light muonic and pionic atoms.

Mechanism	Example	E -dependence	Refs.
Radiative	$(\mu p)_i \rightarrow (\mu p)_f + \gamma$	none	see [1]
External Auger effect	$(\mu p)_i + \text{H}_2 \rightarrow (\mu p)_f + e^- + \text{H}_2^+$	weak	[1, 5]
Stark mixing	$(\mu p)_{nl} + \text{H} \rightarrow (\mu p)_{n'l'} + \text{H}$	moderate	[1, 6–11]
Elastic scattering	$(\mu p)_n + \text{H} \rightarrow (\mu p)_n + \text{H}$	strong	[11–15]
Coulomb transitions	$(\mu p)_{n_i} + p \rightarrow (\mu p)_{n_f} + p, n_f < n_i$	strong	[16–22]
Transfer (isotope exchange)	$(\mu p)_n + d \rightarrow (\mu d)_n + p$	strong	[23–26]
Absorption	$(\pi^- p)_{nS} \rightarrow \pi^0 + n, \gamma + n$	none	see [1]

Table 1: Cascade processes in exotic atoms with $Z = 1$ and their energy dependence.

2 Cascade Mechanisms

A brief summary of the cascade processes in the exotic atoms with $Z = 1$ is given in Table 1. The radiative de-excitation and the nuclear absorption (in hadronic atoms) do not depend on experimental conditions directly. All other processes occur in collisions with surrounding atoms and their rates are proportional to the hydrogen density and usually depend on energy.

At least three cascade mechanisms are essential for the basic understanding of the atomic cascade [1]: the radiative transitions, the external Auger effect, and the Stark mixing. In this paper, the cascade models, which include these three mechanisms only, will be called the minimal cascade model¹ (MCM).

Figure 1 demonstrates the nl -dependence of the total radiative and Auger de-excitation rates for muonic hydrogen. The main features of these de-excitation mechanisms were discussed in [1, 2].

The Auger rates calculated in the Born approximation (Fig. 1b) are energy independent. The eikonal approximation [5] predicts a rather weak energy dependence, with the results being very close to the ones in the Born approximation for $n \leq 6$ and for a kinetic energy of the order of 1 eV. The initial and final state interactions in the Auger transitions were discussed in [17], however, no detailed calculations have been done.

The Stark mixing corresponds to transitions among the nl -sublevels with the same n . It is a very fast collisional process because the exotic atoms

¹In the literature, it has also been called the standard cascade model (SCM).

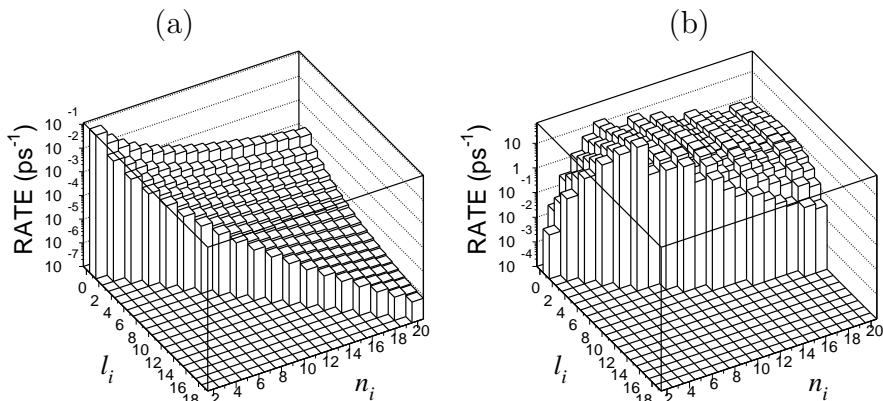


Figure 1: The rates of (a) radiative and (b) Auger de-excitation (LHD) in muonic hydrogen.

with $Z = 1$ are small and electroneutral and have no electrons, so that they can easily pass through the regions of the strong electric field inside ordinary atoms. When the Stark mixing rate is much larger than all other transition rates, the statistical population of the nl -sublevels is determined by the principle of detailed balance.

The relative importance of the various cascade processes in muonic and pionic hydrogen is demonstrated in Figs. 2a,b. The cascade models of the exotic atoms with $Z = 1$ are listed in Table 2; they are of two types. In one group, there are various implementations of the MCM [1, 7, 8, 10] where the kinetic energy is assumed to be constant through the whole cascade. The other group [4, 29–31] consists of detailed kinetics models which take the energy evolution during cascade into account by explicit treatment of acceleration and deceleration mechanisms.

3 X-Ray Yields

Since the rates of the radiative transitions are well known, the competition between the radiative and collisional processes can be used for testing the collisional de-excitation rates by measuring the X-ray yields at various densities. The most suitable system for this study is the muonic hydrogen where the X-ray yields are not suppressed by absorption during the cascade. An-

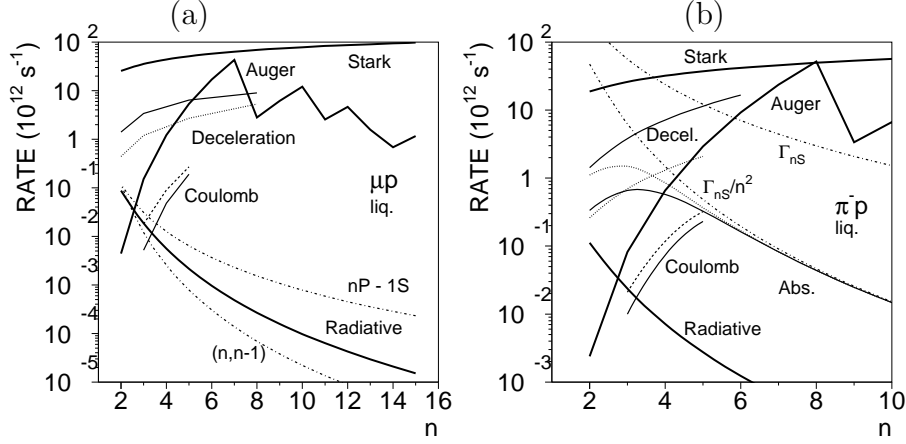


Figure 2: The effective (statistical average) rates for (a) muonic hydrogen [4] and (b) pionic hydrogen [29] in liquid hydrogen. The *effective* absorption rates for the π^-p defined as in [1] and the deceleration rates correspond to the kinetic energy $E = 2$ eV (solid line) and $E = 30$ eV (dotted line). The Coulomb de-excitation rates for $E = 2$ eV (solid line) and $E = 0.04$ eV (dashed line) are from [20, 21].

Model	Systems	Coulomb	Elastic	E -evolution
Leon, Bethe (1962) [1]	π^-p, K^-p	—	—	—
Borie, Leon (1980) [7]	$\mu p, \pi^-p, K^-p, \bar{p}p$	—	—	—
Markushin (1981) [8]	$\mu p, \mu d$	—	—	—
Reinfenröter et al. (1988) [28]	$\bar{p}p$	—	—	—
Czaplinski et al. (1990) [27]	$\mu p, \mu d$	—	—	—
Markushin (1994) [4]	$\mu p, \mu d$	+	+	+
Czaplinski et al. (1994) [26]	$\mu p, \mu d$	+	—	—
Aschenauer et al. (1995) [29, 30]	π^-p	+	+	+
Aschenauer, Markushin (1997) [31]	$\mu p, \mu d$	+	+	+
Terada, Hayano (1997) [10]	$\pi^-p, K^-p, \bar{p}p$	—	—	—

Table 2: The cascade processes included in various models of the lightest exotic atoms in addition to the MCM containing the radiative and Auger de-excitation and the Stark mixing.

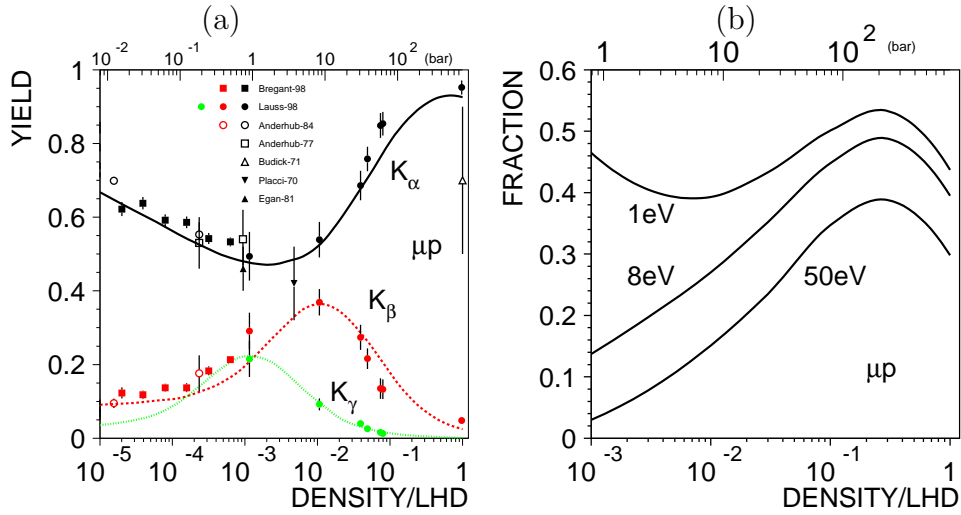


Figure 3: (a) The density dependence of the K_α , K_β , and K_γ yields in muonic hydrogen. The theoretical curves are from [4], the experimental data from [32–39]. (b) The density dependence of the high-energy components ($E \geq 1, 8, 50$ eV) in the μp ground state after the atomic cascade calculated in the model [4] with the Coulomb rates scaled by a factor $k_C = 0.5$ [29].

other convenient factor is that the rates of the Auger de-excitation, which is the main collisional process, have a weak energy dependence, therefore they are not strongly affected by uncertainties in the kinetic energy distribution. The main features of the density dependence of the yields of the K -lines were already fairly well explained by the MCM [7, 8]. Figure 3a shows the experimental data in comparison with the recent calculations [4] that include, in addition to the Auger de-excitation, the Coulomb transitions.

The relative role of the collisional processes can be illustrated by the following simplified calculation of the density dependence of the K_α/K_β ratio using the method suggested in [40]. The yields Y_{K_α} and Y_{K_β} are given by the balance equations:

$$Y_{K_\alpha} \approx p_2 \approx p_3 \frac{\lambda_{3 \rightarrow 2}^\gamma + \phi(\lambda_{3 \rightarrow 2}^{Auger} + \lambda_{3 \rightarrow 2}^{Coulomb})}{\lambda_3^{tot}} \quad (1)$$

$$Y_{K_\beta} = p_3 \frac{\lambda_{3 \rightarrow 1}^\gamma}{\lambda_3^{tot}}, \quad \lambda_3^{tot} = \lambda_{3 \rightarrow 2}^\gamma + \lambda_{3 \rightarrow 1}^\gamma + \phi(\lambda_{3 \rightarrow 2}^{Auger} + \lambda_{3 \rightarrow 2}^{Coulomb}) \quad (2)$$

where p_n are the populations of the atomic states $n = 2, 3$, $\lambda_{3 \rightarrow 1}^\gamma = \lambda_{3P \rightarrow 1S}^\gamma/3$

and $\lambda_{3 \rightarrow 2}^\gamma = \sum_l (2l+1) \lambda_{3l \rightarrow 2P}^\gamma / 9$ are the effective rates of the radiative transitions, ϕ is the hydrogen density in units of liquid hydrogen density $N_0 = 4.3 \cdot 10^{22} \text{cm}^{-3}$ (LHD), $\lambda_{3 \rightarrow 2}^{Auger}$ and $\lambda_{3 \rightarrow 2}^{Coulomb}$ are the rates of the Auger and Coulomb transitions normalized to LHD. Equations (1,2) are valid at $\phi > 0.05$ and give the following dependence of the ratio $Y_{K_\alpha} / Y_{K_\beta}$ on the density:

$$\frac{Y_{K_\alpha}}{Y_{K_\beta}} = \frac{\lambda_{3 \rightarrow 2}^\gamma}{\lambda_{3 \rightarrow 1}^\gamma} + \frac{\phi(\lambda_{3 \rightarrow 2}^{Auger} + \lambda_{3 \rightarrow 2}^{Coulomb})}{\lambda_{3 \rightarrow 1}^\gamma} = 0.79 + 14.6\phi \left(1 + \frac{\lambda_{3 \rightarrow 2}^{Coulomb}}{\lambda_{3 \rightarrow 2}^{Auger}} \right) \quad (3)$$

If one neglects the Coulomb de-excitation, then Eq. (3) gives $(Y_{K_\alpha} / Y_{K_\beta})^{th} = 15$ at $\phi = 1$ which is slightly below the corresponding experimental ratio $(Y_{K_\alpha} / Y_{K_\beta})^{exp} = 19.9 \pm 2.5$ [38]. At $\phi = 0.08$ the difference is larger: $(Y_{K_\alpha} / Y_{K_\beta})^{th} = 2.0$ and $(Y_{K_\alpha} / Y_{K_\beta})^{exp} = 6.4 \pm 1.3$. With the Coulomb transitions taken into account the theoretical ratio gets closer to the experimental values as discussed in [31,38]. This observation can be considered as evidence that some mechanisms in addition to the Auger effect, like the Coulomb transitions, are needed for a better description of the X-ray yields.

4 Kinetic Energy Distribution in Excited States

The evolution of the kinetic energy distribution during the atomic cascade is very important because many collisional processes are energy dependent (Table 1). In muonic atoms, it determines the initial energy distribution in the ground state, which influences the diffusion of μ -atoms [41–43] and muon catalyzed fusion [44,45]. A large fraction of the atoms is not thermalized² during the atomic cascade, as it follows from the cascade calculation demonstrated in Fig.3b.

The kinetic energy distribution in the atomic cascade can be studied with different methods. Direct probes which are model independent are based on the measurements of the Doppler broadening of the X-ray lines in μp and $\pi^- p$ and the n -TOF spectra in the reaction $\pi^- p \rightarrow \pi^0 + n$. Given the kinetic energy distribution $w(E)$ at the instant of the radiative transition, the Doppler broadening of the X-ray line $g(\Delta\omega)$ has the form:

$$g(\Delta\omega) = \frac{1}{2\xi} \int_{(\Delta\omega/\xi)^2}^{\infty} \frac{w(E)}{\sqrt{E}} dE, \quad \xi = \frac{\omega_0}{c} \sqrt{\frac{2}{M}} \quad (4)$$

²The atoms with the kinetic energy much larger than the temperature are called epithermal and the ones with $E \gg 1 \text{ eV}$ — 'hot' or 'highly-energetic'.

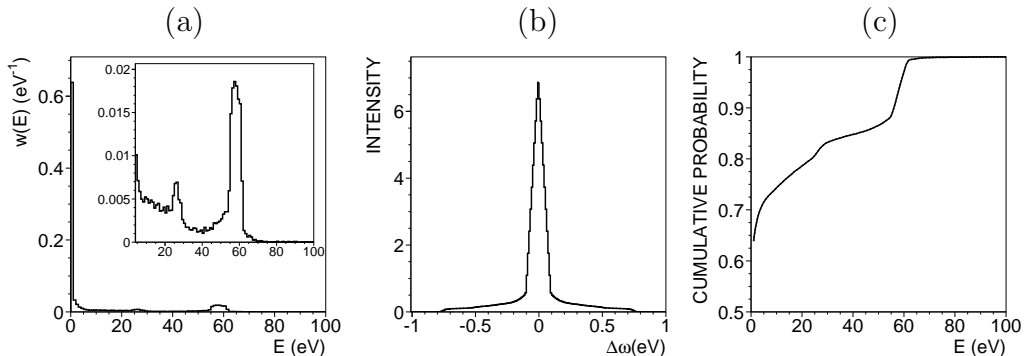


Figure 4: (a) The kinetic energy distribution $w(E)$ at the instant of the $3P \rightarrow 1S$ transition in muonic hydrogen at 15 bar, (b) the corresponding Doppler broadening of the K_β line and (c) the cumulative energy distribution $W(E)$.

where ω_0 is the X-ray energy in the atomic rest frame and M is the mass of the atom. A straightforward inversion of the transformation (4) gives the cumulative energy distribution $W(E)$:

$$W(E) \stackrel{def}{=} \int_0^E w(E') dE' = 2 \int_0^{\xi\sqrt{E}} g(x) dx - 2\xi\sqrt{E}g(\xi\sqrt{E}) \quad . \quad (5)$$

Figure 4 shows an example of the calculated distributions for the K_β -transition in μp atoms at 15 bar which features characteristic peaks in the high-energy component resulting from the Coulomb de-excitation discussed in Sec. 6. The Doppler broadening of the neutron TOF spectra from the reaction $(\pi^- p) \rightarrow \pi^0 + n$ is related to the kinetic energy distribution in a similar way (see [46–48]). A good knowledge of the kinetic energy distribution is essential for precise measurements of the $(\pi^- p)_{1S}$ nuclear width [49]. For example, the kinetic energy $T = 0.5$ eV corresponds to a Doppler broadening of the K_β line $\delta\Gamma = 0.1$ eV which is about 10% of the nuclear width $\Gamma_{1S} = 1$ eV.

Indirect methods of probing the kinetic energy distribution rely on models of the kinetics. In particular, the first evidence for epithermal muonic atoms was found in muon catalyzed fusion (see [45] and references therein). Important results on the initial kinetic energy distribution in the ground state were obtained from the diffusion of μp and μd atoms at low density [41–43]; they allow one to determine the energy distribution in excited states using cascade models as discussed in [4, 43]. Indirect methods exploiting energy

dependent processes, like the muon transfer in excited states [26,50,51], were used for the estimates of the average energy in excited states, however, they are not sensitive to the details of the energy distributions.

5 Elastic Collisions

The elastic collisions, where the principal quantum number of the exotic atom is not changed, play two important roles in the atomic cascade. First, the Stark mixing is nothing but the elastic scattering as long as only the rates of transitions between the l -sublevels of the same n are concerned. Second, the energy losses in elastic collisions lead to the deceleration of the epithermal exotic atoms.

The basic features of the elastic scattering can be explained in the semi-classical approximation [23]. The motion of the μp atom with the parabolic quantum numbers (n_1, n_2, m) in the electric field of a hydrogen atom is described by the effective potential³

$$V(R) = \frac{g}{R^2} \zeta(R/a), \quad g = \frac{3n\Delta}{2m_{\mu p}} \quad (6)$$

where $\Delta = (n_1 - n_2)$, $m_{\mu p}$ is the μp reduced mass, $\zeta(r) = (1 + 2r + 2r^2)e^{-2r}$ is the electron screening factor, a is the electron Bohr radius. Neglecting the electron screening, this corresponds to the well known R^{-2} potential with a large dimensionless coupling constant $2Mg = \frac{3}{2}n\Delta M/m_{\mu p} \sim Mn^2/m_{\mu p} \gg 1$ (M is the reduced mass of the $\mu p + p$ system). The R^{-2} behaviour leads to the E^{-1} dependence of the elastic cross section. In the limit $2Mg \gg 1$, many partial waves contribute to the scattering, and the differential cross section can be approximated by the classical result ($g > 0$):

$$\frac{d\sigma(E, \theta)}{d\Omega} = \frac{\pi g}{E} w(\theta) \quad (7)$$

$$w(\theta) = \frac{\pi(\pi - \theta)}{(2\pi - \theta)^2 \theta^2 \sin \theta} \approx \frac{1}{32 \sin^3 \theta/2} \quad (8)$$

The average coupling constant for given n is $g = (n^2 - 1)/2m_{\mu p}$. The cross section (7,8) has an unphysical singularity at $\theta \rightarrow 0$ which must be regularized by taking the electron screening into account.

³The quantization axis is along the electric field, $n = n_1 + n_2 + |m| + 1$.

A semiclassical model of the Stark mixing was developed in [1] and used with some variations and refinements in [6–8, 10]. In this model, the exotic atom moves along a straight line trajectory with a constant velocity through the electric field of a hydrogen atom, and the Stark transitions induced by this electric field are calculated. Instead of straight line trajectories the classical trajectories can be used as in [28]. The characteristic scale of the Stark mixing cross section is determined by the electron screening of the proton electric field, i.e. by the size of the hydrogen atom which makes Stark mixing the fastest collision process in the atomic cascade, see Figs. 2.

Recently the problem of the elastic scattering of exotic atoms in excited states was treated in a quantum mechanical framework using the adiabatic expansion [9, 11, 15], the calculation being done in a single-channel adiabatic approximation. The results show fair agreement with the semiclassical calculations [14] for the collision energies $E > 1$ eV. A detailed discussion of the Stark collisions, including the relative role of transitions with different $\Delta l = l_f - l_i$ can be found in [11]. It would be desirable to extend the quantum mechanical model of the elastic collisions by including the effects of the shift and width of the nS states as well as the coupling between different adiabatic terms.

The elastic scattering leads to the deceleration of exotic atoms if the kinetic energy is larger than the target temperature. The effective deceleration rate for the $\mu p + p$ collisions is defined by the transport cross section:

$$\lambda_n^{dec}(E) = N_0 v \frac{2 M_{\mu p} M_H}{(M_{\mu p} + M_H)^2} \sigma_n^{tr}(E), \quad (9)$$

$$\sigma_n^{tr}(E) = \int (1 - \cos \theta) d\sigma_n(E, \theta) \quad (10)$$

where v is the atomic velocity, $M_{\mu p}$ and M_H are the μp and hydrogen masses correspondingly. Using the classical result (7,8) one gets the following estimation⁴ of the transport cross section:

$$\sigma_n^{tr}(E) \approx \frac{\pi^2 (n^2 - 1)}{4m_{\mu p} E}. \quad (11)$$

The deceleration rate (Fig. 2) is a crude measure of the slowing down; in general one uses the differential cross sections in detailed kinetics calculations. The first estimation of the deceleration rates was done in [12], semiclassical

⁴Note that the transport cross section is finite even without the electron screening.

calculations were done in [13, 14], and quantum mechanical calculations in [9, 11, 15].

6 Coulomb De-excitation

The Coulomb de-excitation (Table 1), where the transition energy is shared between the colliding particles, is an important acceleration mechanism producing 'hot' ($E \gg 1$ eV) exotic atoms (see Fig. 4a). The highly-energetic π^-p atoms were discovered experimentally in [52], and a multicomponent structure of the energy distribution was found in [46]. Recent experiments in liquid and gaseous hydrogen [47, 48] found the shape of the kinetic energy distribution to be consistent with the Coulomb mechanism. The cascade calculations [29] show that the π^-p atoms with kinetic energy $E \geq 50$ eV are not significantly decelerated between the Coulomb de-excitation and the nuclear reaction. For the atoms with $E \leq 20$ eV the deceleration is important and the Coulomb peaks are expected to be smeared out.

The earlier calculations of the Coulomb transitions [16–19] were rather controversial. The latest calculations [20–22] seem to clarify the theoretical picture. This removes one of the uncertainties in the cascade calculation of the past where a Coulomb rate-tuning parameter was used to normalize the calculated high-energy component to the measurements in pionic hydrogen [29]. It is not excluded that the Coulomb de-excitation can be part of a multistep process. For instance, the formation of excited molecular states can be followed by a Coulomb-like decay [2, 54, 55].

7 Atomic Cascade in H-D Mixtures

The atomic cascade in mixtures of hydrogen isotopes provides additional information on the collisional processes in excited states. The muon transfer in excited states was studied in detail in the recent experiments [50, 51, 53] by measuring the relative yields of the μp and μd K -lines in liquid and gaseous HD mixtures. Figure 5 shows a comparison of the experimental data with the cascade calculations for the probability Q_{1S} that the muon captured initially by the hydrogen in a HD mixture reaches the μp ground state (the fraction $(1 - Q_{1S})$ is transferred to μd during the atomic cascade). Since the rates of the muon transfer $(\mu p)_n + d \leftrightarrow (\mu d)_n + p$ are strongly energy

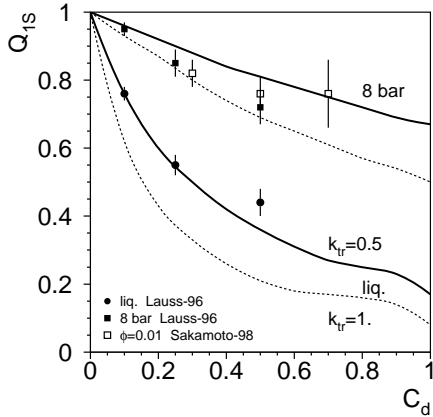


Figure 5: The Q_{1S} factor for the μp cascade in HD mixture vs. deuterium fraction C_d . The data are from [50, 53]; the theoretical curves [31] were calculated with the transfer rates [25] scaled by the factor $k_{tr} = 0.5$ (solid lines) and $k_{tr} = 1$ (dashed lines).

dependent [23–26], the Q_{1S} factor is very sensitive to the kinetic energy distribution in the excited states [2, 24, 26, 27, 31].

The theoretical models tend to predict a stronger dependence of Q_{1S} on the deuterium fraction and the density than experimentally observed (this so-called “ Q_{1S} -problem” is known since the first experimental results were obtained from the kinetic analysis of muon catalyzed fusion [44, 45]). The agreement between theory and experiment improves if the transfer rates are scaled by a factor of about 0.5 [31]. This suggests that some mechanism may still be missing in the cascade model. One candidate is the resonant molecular formation in excited states (resonance side-path mechanism [55]) which can produce a significant inverse transfer $\mu d \rightarrow \mu p$ leading to an enhancement of Q_{1S} as discussed in [56].

8 Conclusion

The current cascade models are advancing from a phenomenological level towards straightforward detailed calculations of the kinetics. The recent progress in quantum mechanical calculations of the scattering of exotic atoms in excited states makes it possible to get rid of tuning parameters and ad hoc assumptions in future calculations. The ultimate goal of *ab initio* cascade

calculations does not seem to be unrealistic any more.

A detailed knowledge of atomic cascade is essential for precision X-ray spectroscopy of the π^-p atom where the Doppler-broadening corrections must be taken into account in order to measure the nuclear width of the $1S$ state. The new generation of precise experiments with the μp and π^-p atoms [49] will make it possible to study the kinetics of the atomic cascade in great detail and to perform critical tests of the theoretical methods used in the calculations of various reactions with excited exotic atoms. The results of these studies will also be very useful for other systems like K^-p and $\bar{p}p$.

Acknowledgements

The author thanks A. Badertscher, M. Daum, P. Froelich, P.F.A. Goudsmit, F. Kottmann, B. Lauss, H.J. Leisi, L.I. Ponomarev, V.P. Popov, J. Schottmüller, L.M. Simons, E.A. Solov'ev, D. Taqqu, and J. Wallenius for fruitful discussions.

References

- [1] M. Leon and H.A. Bethe, Phys. Rev. **127** (1962) 636.
- [2] V.E. Markushin, in *EM Cascade and Chemistry of Exotic Atoms*, Eds. L.M. Simons et al., Plenum, NY, 1990, p. 73.
- [3] F. Kottmann, in *Muonic Atoms and Molecules*, Eds. L.A. Schaller and C. Petitjean, Birkhäuser, Basel, 1993, p. 219.
- [4] V.E. Markushin, Phys.Rev. **A50** (1994) 1137.
- [5] A.P. Bukhvostov and N.P. Popov, Sov. Phys. JETP **55** (1982) 12.
- [6] J.-L. Vermeulen, Nucl. Phys. **B12** (1969) 506.
- [7] E. Borie and M. Leon, Phys. Rev. **A21** (1980) 1460.
- [8] V.E. Markushin, Sov. Phys. JETP **53** (1981) 16 [ZhETF **80** (1981) 35].
- [9] V.P. Popov and V.N. Pomerantsev, Hyperfine Interactions **101/102** (1996) 133.

- [10] T.P. Terada and R.S. Hayano, Phys. Rev. C **55** (1997) 73.
- [11] V.P. Popov and V.N. Pomerantsev, these proceedings.
- [12] L.I. Menshikov and L.I. Ponomarev, Z. Phys. D **2** (1986) 1.
- [13] W. Czaplinski et al., Hyperfine Interactions **101/102** (1996) 151.
- [14] V. Bystritsky et al., Phys. Rev. A **53** (1996) 4169.
- [15] V.P. Popov, V.N. Pomerantsev, and V.V. Gusev, these proceedings.
- [16] L. Bracci and G. Fiorentini, Nuovo Cim. **43A** (1978) 9.
- [17] L.I. Menshikov, Muon Catalyzed Fusion **2** (1988) 173.
- [18] W. Czaplinski et al., Muon Catalyzed Fusion **5/6** (1990/91) 59.
- [19] W. Czaplinski et al., Phys. Rev. A **50** (1994) 525.
- [20] L.I. Ponomarev and E.A. Solov'ev JETP Lett. 64 (1996) 135.
- [21] E.A. Solov'ev, these proceedings.
- [22] A.V. Kravtsov, these proceedings.
- [23] L.I. Menshikov and L.I. Ponomarev, JETP Letters **39** (1984) 663.
- [24] A.V. Kravtsov, Muon Catalyzed Fusion **2** (1988) 183.
- [25] V.V. Gusev et al.: Hyperfine Interactions **82** (1993) 53.
- [26] W. Czaplinski et al., Phys. Rev. A **50** (1994) 518.
- [27] W. Czaplinski, Muon Catalyzed Fusion **5/6** (1990/91) 55.
- [28] G. Reinfenröter et al., Phys. Lett. **214B** (1988) 325.
- [29] E.C. Aschenauer et al., Phys. Rev. **A51** (1995) 1965.
- [30] A.J. Rusi El Hassani et al., Z. Phys. **A351** (1995) 113.
- [31] E.C. Aschenauer and V.E. Markushin, Z. Phys. D **39** (1997) 165.
- [32] A. Placci et al., Phys. Lett. **32B** (1970) 413.

- [33] B. Budick et al., Phys. Lett. **34B** (1971) 539
- [34] H. Anderhub et al., Phys. Lett. **71B** (1977) 433.
- [35] P.O. Egan et al., Phys. Rev. **A23** (1981) 1152.
- [36] A. Anderhub et al., Phys. Lett. **101B** (1981) 151.
- [37] A. Anderhub et al., Phys. Lett. **143B** (1985) 65.
- [38] B. Lauss et al., Phys. Rev. Lett. **80** (1998) 3041.
- [39] M. Bregant et al., Phys. Lett. A **241** (1998) 344.
- [40] V.E. Markushin, Sov. J. Nucl. Phys. **40** (1984) 612.
- [41] D.J. Abbott et al., Phys. Rev. A **55** (1997) 165.
- [42] F.J. Hartmann et al., Hyperfine Interactions **101/102** (1996) 623.
- [43] F. Kottmann, these proceedings.
- [44] L.I. Ponomarev, Contemp. Phys. 31 (1991) 218.
- [45] J.S. Cohen, in *Review of Fundamental Processes and Applications of Atoms and Ions, Ch. 2*, Ed. C.D. Lin, World Scientific, Singapore, 1994.
- [46] J.E. Crawford et al. Phys. Lett. **213B** (1988) 391; Phys. Rev. **D43** (1991) 46.
- [47] A. Badertscher et al., Phys. Lett. **B 392** (1997) 278.
- [48] J. Schottmüller et al., these proceedings.
- [49] L.M. Simons, these proceedings.
- [50] B. Lauss et al., Phys. Rev. Lett. **76** (1996) 4693.
- [51] B. Lauss et al., these proceedings.
- [52] J.B. Czirr, Phys. Rev. **130** (1963) 341.
- [53] S. Sakamoto et al., these proceedings.

- [54] D. Taqqu, in AIP Conf. Proc. 181, p. 217, Eds. S.E. Jones et al., AIP, NY, 1989.
- [55] P. Froelich and J. Wallenius, Phys.Rev.Lett **75** (1995) 2108.
- [56] J. Wallenius and P. Froelich, these proceedings.